Supporting Information

Hydrothermal aging effects on NH_3 oxidation over high-loading Cu-SSZ-13 catalyst: An experimental and kinetic modeling study

Minghui Rui,[a] Meiqing Shen,[acd] Wei Li,[c] Feng Gao,[cd] Liwei Jia,[c] Xinhua Li [ce] and Gurong Shen *[b]

[a] School of Chemical Engineering and Technology, Tianjin University, Tianjin 300350, China
[b] School of Materials Science and Engineering, Tianjin University, Tianjin 300350, China
[c] National Rare Earth Catalysis Research Institute, Dongying 257000, China
[d] State Key Laboratory of Engines, Tianjin University, Tianjin 300072, China
[e] Shandong Institute of Petroleum and Chemical Technology, Dongying 257061, China

*Corresponding author.
E-mail address: gr_shen@tju.edu.cn

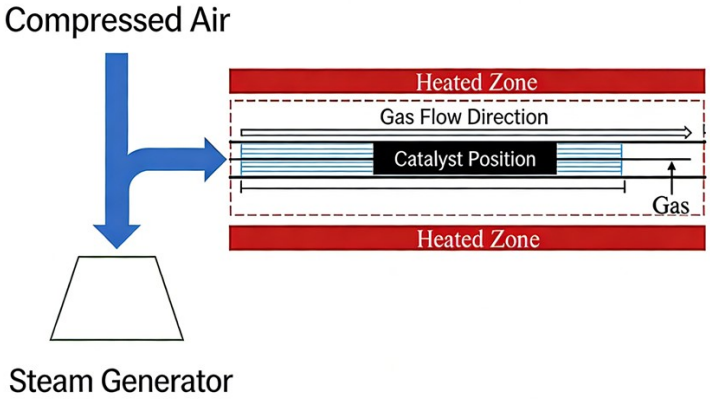

Fig. S1. Schematic diagram of the tube furnace setup for hydrothermal aging.

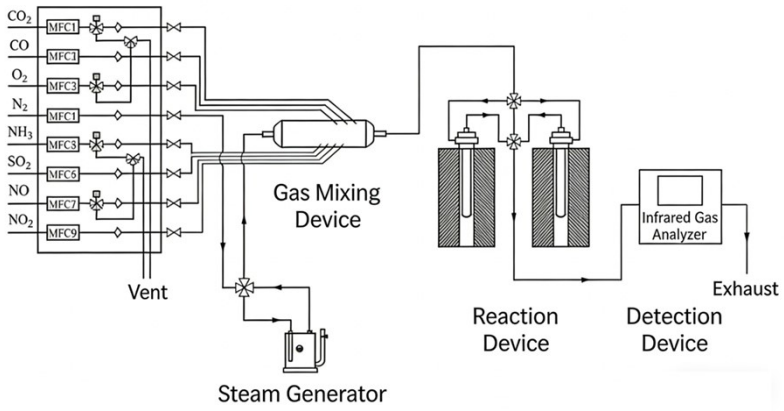

Fig. S2. Schematic diagram of the homemade evaluation system.

Table S1. Cu content of different samples from ICP.

Samples	Fresh	600-16h	650-16h	700-16h	800-16h
Cu (wt.%)	3.83	3.83	3.83	3.83	3.83

ICP results in Table S1 show that the Cu content of all samples remains consistent with that of the fresh sample (3.83 wt.%).

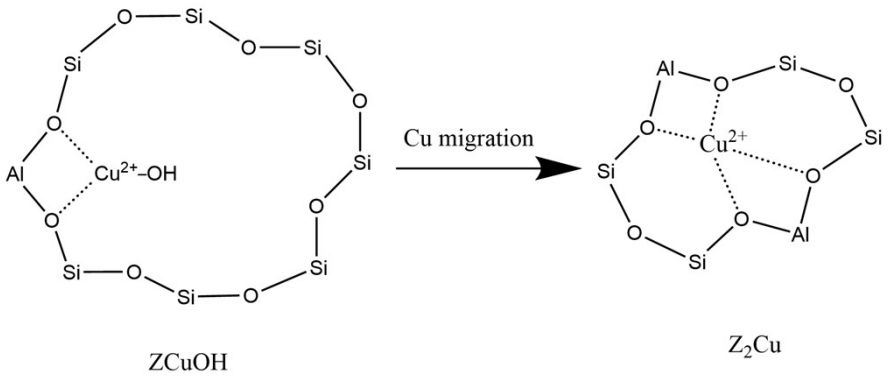

Fig. S3. Different positions of ZCuOH and Z_2Cu and the Cu migration process.

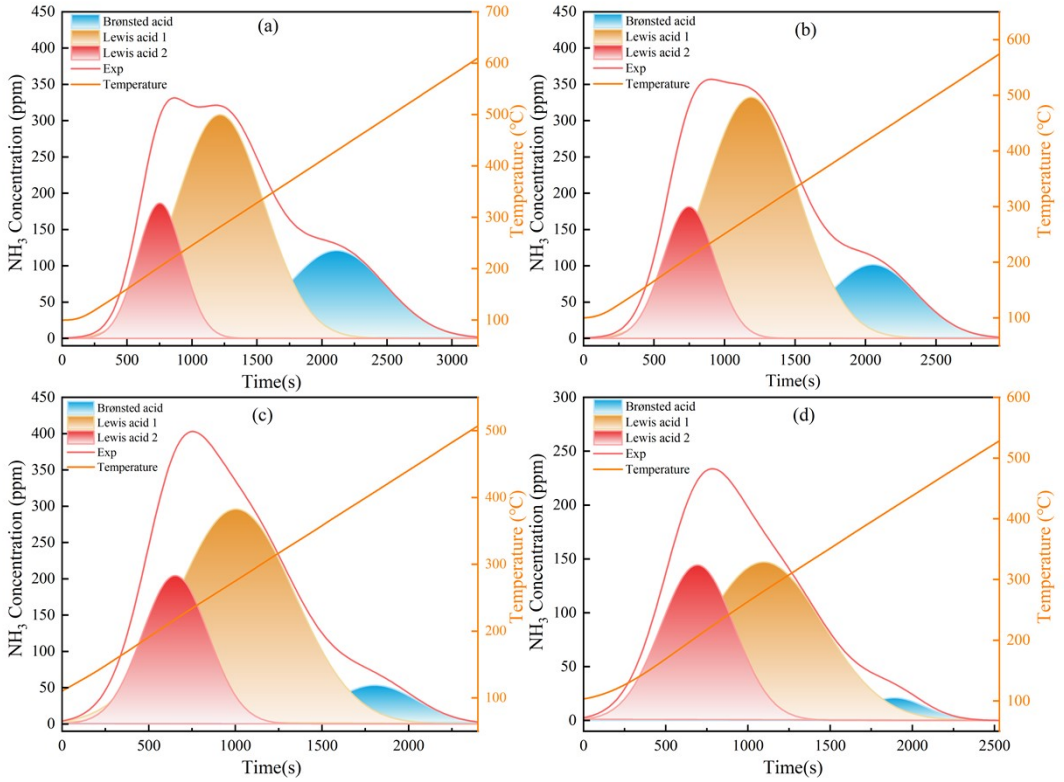

Fig. S4. Peak fitting results of NH_3-TPD over different aged samples. (a) 600-16h sample; (b) 650-16h sample; (c) 700-16h sample; (d) 800-16h sample.

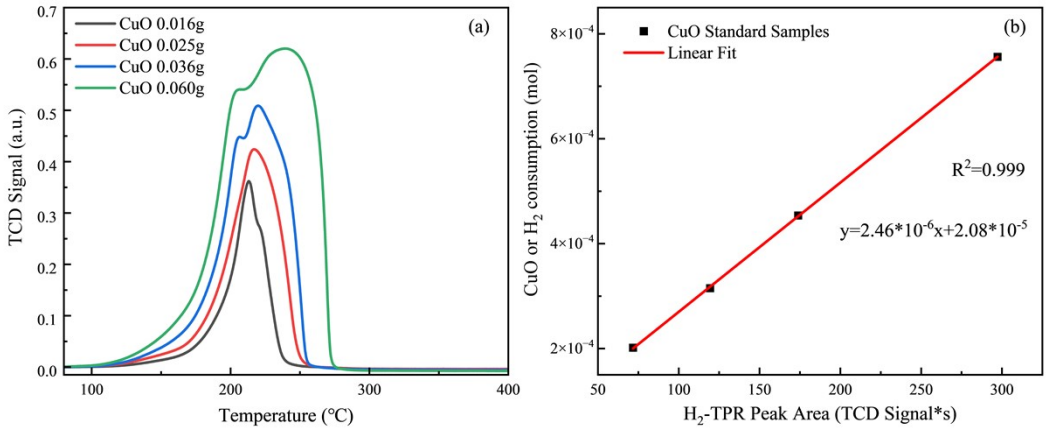

Fig.S5. (a) H_2-TPR results over CuO standard samples. (b) The linear relationship between H_2-TPR peak area (TCD Signal*s) and CuO or H_2 consumption.

As shown in Fig. S5, there are two reduction peaks attributed to R2 and R3, respectively. Additionally, a linear relationship between H_2-TPR peak area (TCD Signal*s) and H_2 consumption was established, providing a calibration factor for subsequent quantitative work.

$$CuO + H_2 = Cu + H_2O\#(1)$$

$2Cu^{II}O + H_2 \rightarrow Cu^{I}{}_2O + H_2O\#(2)$

$Cu^{I}{}_2O + H_2 \rightarrow 2Cu^0 + H_2O\#(3)$

The abscissa (temperature) in Fig. 5 was converted to time (s). After removing the instrument-provided baseline, the peaks below 450 °C were integrated to obtain the TCD Signal*s values. Subsequently, the actual H_2 consumption (below 450 °C) was calculated using the calibration curve $y=2.46*10^{-6}x+2.08*10^{-5}$ (Fig. S5), and the results are listed in Table S2.

Table S2. H_2 consumption below 450 °C of different samples. (0.3 g catalyst)

Samples	Fresh	600-16h	650-16h	700-16h	800-16h
H_2 consumption (μmol)	103	98	99	106	110

The theoretical H_2 consumption was calculated based on the stoichiometric ratio of the relevant reduction reaction. According to reaction equations R4 ($ZCu^{II}OH + \frac{1}{2}H_2 \rightarrow ZCu^{I} + H_2O$) and R5 ($Z_2Cu^{II} + \frac{1}{2}H_2 \rightarrow ZCu^{I} + ZH$). 1 mole of Cu^{2+} consumes 0.5 moles of H_2. In contrast, 1 mole of CuO consumes 1 mole of H_2. Taking the fresh catalyst sample as an example: the catalyst contains Cu^{2+} at a content of 3.07 wt.% (equivalent to 483.7 μmol/g) and CuO at a content of 0.76 wt.% (equivalent to 95.1 μmol/g). The theoretical H_2 consumption of 0.3 g catalyst is calculated as follows:

H_2 consumption = (483.7/2+95.1）*0.3=101 (μmol）

By the same token, the theoretical H_2 consumption of 800-16h sample is calculated to be 115 (μmol). Notably, the theoretical H_2 consumption values derived from stoichiometric ratio calculations are in good agreement with the experimental results presented in Table S2.

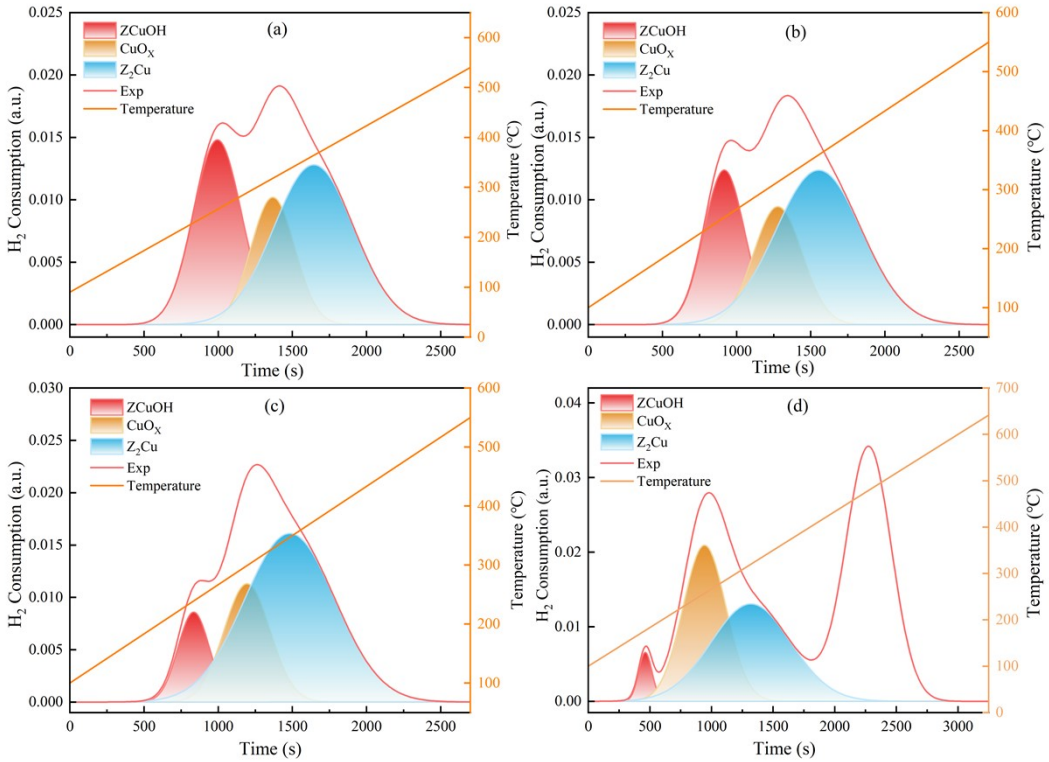

Fig.S6. Experimental and peak fitting of H_2-TPR results. (a) 600-16h sample; (b) 650-16h sample; (c) 700-16h sample; (d) 800-16h sample.

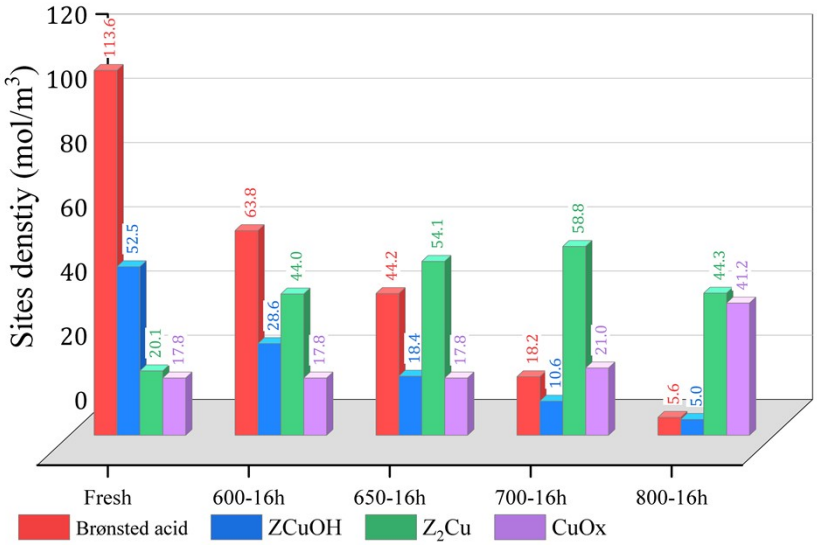

Fig. S7. Site density at different sites of fresh catalyst and different aged samples.

Based on the results of NH_3-TPD, NO+NH_3 titration, and H_2-TPR, it is known that when the coating amount is 150g/L, the site density of each site can be calculated, which provides a basis for model establishment.

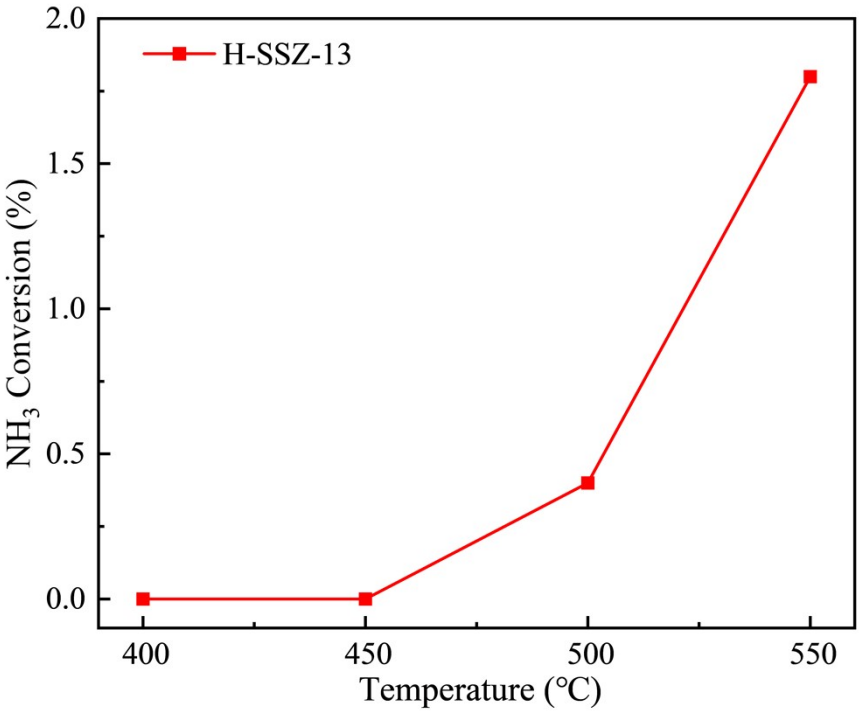

Fig.S8. NH_3 oxidation results of H-SSZ-13. 100 mg catalyst was used; GHSV=100,000 h^{-1}, NH_3=500 ppm, O_2=10%， H_2O=3.8%, N_2 balance.

As shown in Fig. S8, NH_3 oxidation tests under same conditions were conducted over the model catalyst H-SSZ-13, which exhibited negligible NH_3 conversion in the low-temperature range.

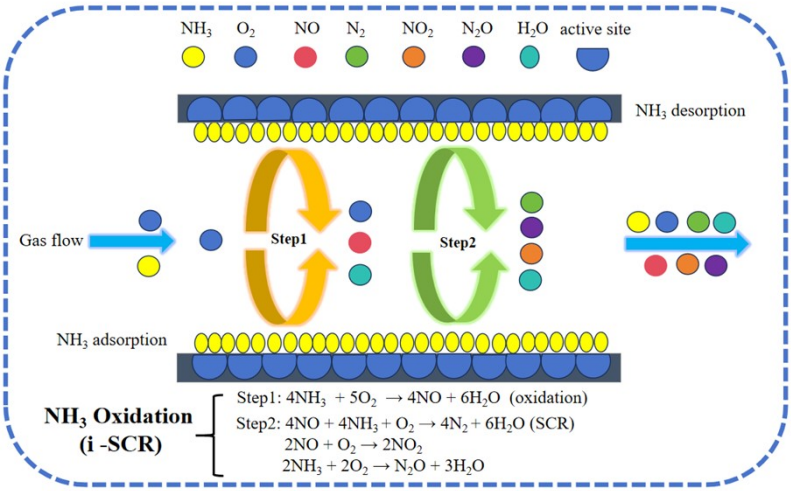

Fig. S9. Schematic diagram of NH_3-SCO mechanism.

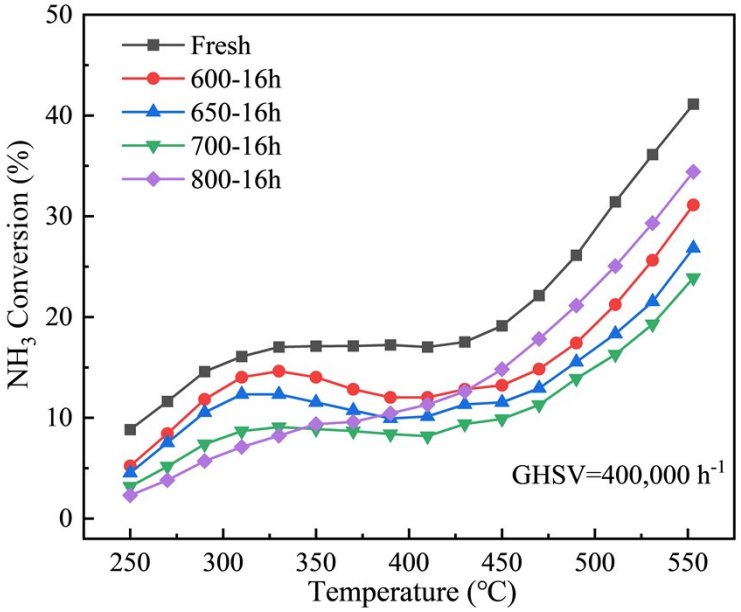

Fig. S10. Steady state NH_3 oxidation reaction results over fresh sample and different aged samples. 33 mg catalyst was used; GHSV=400,000 h^{-1}, NH_3=500 ppm, O_2=10%， H_2O=3.8%, N_2 balance.

In steady-state curves, all samples exhibit two distinct kinetic regimes similar to those in Fig. 7(a).

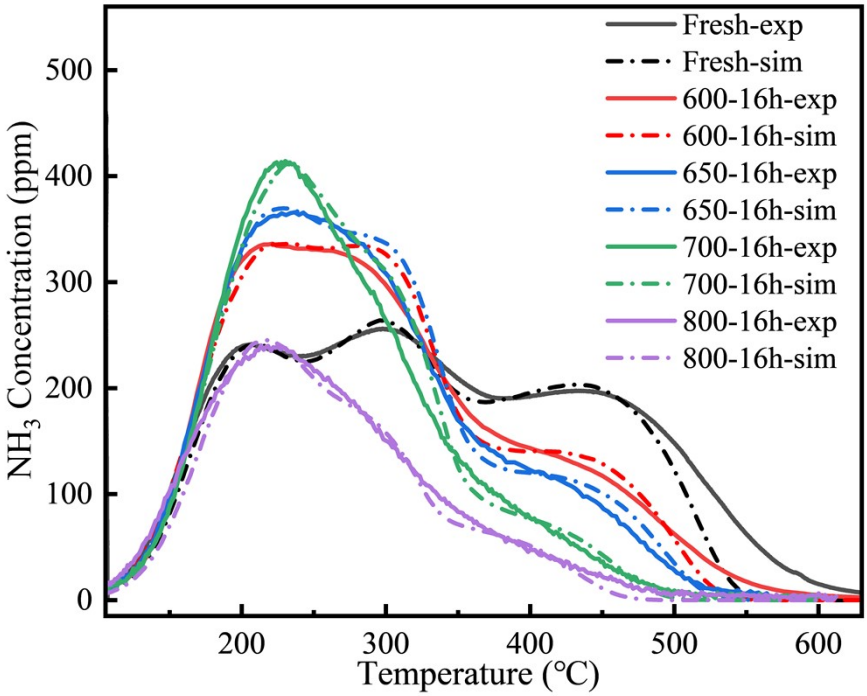

Fig. S11. Experimental and simulation results of NH_3-TPD over fresh and different aged samples.

A comparison of the experimental and simulated NH_3-TPD desorption profiles demonstrates that the developed model successfully predicts the NH_3 desorption

behaviour of the fresh catalyst samples. Furthermore, with the kinetic parameters fixed, merely adjusting the active site density enabled the model to accurately reproduce the variation trends in both the position and intensity of the NH_3 desorption peaks for the hydrothermally aged samples. These results collectively validate the rationality and reliability of the NH_3-TPD model established in this study.

Nomenclature

Nomenclature	
t	Time (s)
T	Temperature (K)
R	Ideal gas constant ($J \cdot mol^{-1} \cdot K^{-1}$)
r_j	Reaction rate for reaction j ($mol/m^3 \cdot s$)
k_j	Rate constant for reaction j (s^{-1})
A_j	Pre-exponential factor for reaction j (s^{-1})
$E_{a,j}$	Activation energy of reaction j (kJ/mol)
$E_{a,j}^{0}$	Activation energy for reaction j at zero coverage (kJ/mol)
α_j	Coverage dependence in reaction j (-)
Ω_k	Site density of active site k (mol/m^3)
$\theta_{i,k}$	Coverage of species i on storage site k (-)
$y_{i,k}$	Volume fraction at the reaction layer of specie i (-)